almost constant after 45 min, and the particle number was almost constant during polymerization.

From these results, the polymerization using a fast-decomposing initiator at high temperature improves the diameter distribution of the particles obtained owing to the short particle formation period. The optimization of polymerization condition (reaction temperature: 343→353 K, initiator: AIBN→ADVN) successfully reduced the CV of the particles to 9.1 from 23.6% [Fig. 6(b)].

CONCLUSIONS

In dispersion copolymerization of styrene with VBA-PAspNa in a mixture of ethanol and water, polymerization parameters such as water contents in media, initiator concentration, styrene monomer concentration, reaction temperature, and type of initiator affected the particle diameter and the diameter distribution. The particle diameter greatly decreased and CV slightly increased with increasing water contents in the media. Particle diameter increased with increasing initiator concentration. The period of increase of CV and particle number, namely, the period of particle formation increased with increasing styrene monomer concentration. From this result, we found that the particle diameter distribution in the final particles was determined by the nucleation period. Monodispersity of the particles can be improved by shortening of the decomposition time of initiator, which is determined by the reaction temperature and the molecular structure.

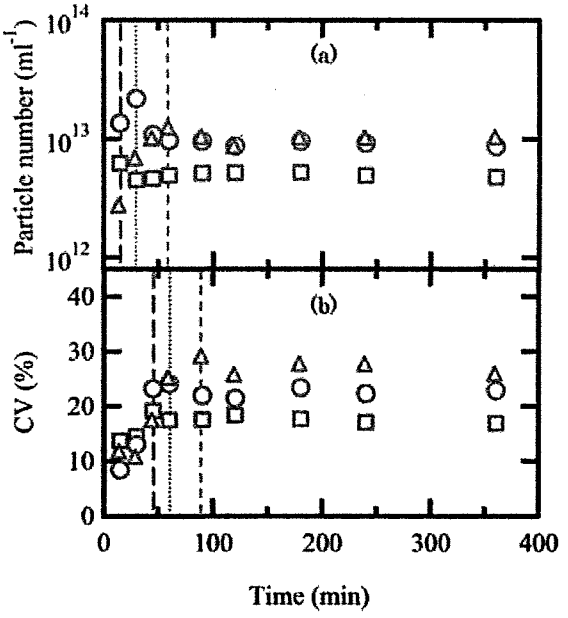

Figure 7. Time courses of (a) particle number and (b) CV in dispersion copolymerization at different reaction temperature: 333 K (△, - - -), 343 K (○, ·····), 353 K (□, – – –). The lines indicate the times for maximum values of the particle number and CV during polymerization.

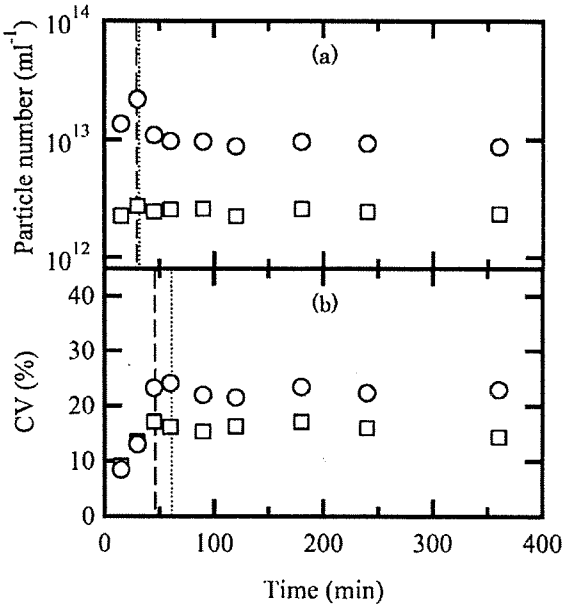

Figure 8. Time courses of (a) particle number and (b) CV in dispersion copolymerization with AIBN (○, ·····), ADVN (□, – – –) as an initiator. The lines indicate the times for maximum values of the particle number and CV during polymerization.

REFERENCES AND NOTES

1. Sakuma, S.; Hayashi, M.; Akashi, M. Adv Drug Delivery Rev 2001, 47, 21–37.
2. Amalvy, J. I.; Unali, G.-F.; Li, Y.; Granger-Bevan, S.; Armes, S. P. Langmuir 2004, 20, 4345–4354.
3. Mei, Y.; Lu, Y.; Polzer, F.; Ballauff, M. Chem Mater 2007, 19, 1062–1069.
4. Zhao, B.; Jiang, X.; Li, D.; Jiang, X.; O'Lenick, T. G.; Li, B.; Li, C. Y. J Polym Sci Part A: Polym Chem 2008, 46, 3438–3446.
5. Yasui, M.; Shiroya, T.; Fujimoto, K.; Kawaguchi, H. Colloids Surf B: Biointerf 1997, 8, 311–319.
6. Tsuji, S.; Kawaguchi, H. Langmuir 2005, 21, 2434–2437.
7. Tsuji, S.; Kawaguchi, H. e-Polymer 2005, 76, 1–7.

8. Uyama, H.; Honda, Y.; Kobayashi, S. J Polym Sci Part A: Polym Chem 1993, 31, 123–128.
9. Ito, K.; Sabao, K.; Kawaguchi, S. Macromol Symp 1995, 91, 65–72.
10. Brown, R.; Stützel, B.; Sauer, T. Macromol Chem Phys 1995, 196, 2047–2064.
11. Kawaguchi, S.; Tano, K.; Maniruzzaman, M.; Ito, K. Macromol Symp 2000, 150, 101–108.
12. Shen, R.; Akiyama, C.; Senyo, T.; Ito, K. C R Chimie 2003, 6, 1329–1335.
13. Kobayashi, S.; Uyama, H.; Lee, S. W.; Matsumoto, Y. J Polym Sci Part A: Polym Chem 1993, 31, 3133–3139.
14. Kawaguchi, S.; Winnik, M. A.; Ito, K. Macromolecules 1995, 28, 1159–1166.
15. Lacroix-Desmazes, P.; Guyot, A. Polym Bull 1996, 37, 183–189.
16. Furuhashi, H.; Kawaguchi, S.; Itsuno, S.; Ito, K. Colloid Polym Sci 1997, 275, 227–233.
17. Capek, I.; Riza, M.; Akashi, M. J Polym Sci Part A: Polym Chem 1997, 35, 3131–3139.
18. Liu, J.; Gan, L. M.; Chew, C. H.; Quek, C. H.; Gong, H.; Gan, L. H. J Polym Sci Part A: Polym Chem 1997, 35, 3575–3583.
19. Chen, M.-Q.; Serizawa, T.; Kishida, A.; Akashi, M. J Polym Sci Part A: Polym Chem 1999, 37, 2155–2166.
20. Chudej, J.; Guyot, A.; Capek, I. Macromol Symp 2002, 179, 241–256.
21. Tomita, K.; Ono, T. J Polym Sci Part A: Polym Chem 2009, 47, 762–770.
22. Neri, P.; Antoni, G.; Benvenuti, F.; Cocola, F.; Gazzei, G. J Med Chem 1973, 16, 893–897.
23. Nakato, T.; Tomida, M.; Suwa, M.; Morishima, Y.; Kusuno, A.; Kakuchi, T. Polym Bull 2000, 44, 385–391.
24. Suwa, M.; Hashidzume, A.; Morishima, Y.; Nakato, T.; Tomida, M. Macromolecules 2000, 33, 7884–7892.
25. Kang, H. S.; Yang, S. R.; Kim, J.-D.; Han, S.-H.; Chang, I.–S. Langmuir 2001, 17, 7501–7506.
26. Lok, K. P.; Ober, C. K. Can J Chem 1985, 63, 209–216.
27. Tseng, C. M.; Lu, Y. Y.; El-Aasser, M. S.; Vanderhoff, J. W. J Polym Sci Part A: Polym Chem Ed 1986, 24, 2995–3007.
28. Paine, A. J.; Luymes, W.; McNulty, J. Macromolecules 1990, 23, 3104–3109.
29. Chen, Y.; Yang, H.-W. J Polym Sci Part A: Polym Chem 1992, 30, 2765–2772.
30. Kobayashi, S.; Uyama, H.; Matsumoto, Y.; Yamamoto, I. Makromol Chem 1992, 193, 2355–2362.
31. Shen, S.; Sudol, E. D.; El-Aasser, M. S. J Polym Sci Part A: Polym Chem 1993, 31, 1393–1402.
32. Tuncel, A.; Kahraman, R.; Piskin, E. J Appl Polym Sci 1993, 50, 303–319.
33. Hattori, M.; Sudol, E. D.; El-Aasser, M. S. J Appl Polym Sci 1993, 50, 2027–2034.
34. Shen, S.; Sudol, E. D.; El-Aasser, M. S. J Polym Sci Part A: Polym Chem 1994, 32, 1087–1100.
35. Thomson, B.; Rudin, A.; Lajoie, G. J Polym Sci Part A: Polym Chem 1995, 33, 345–357.
36. Cao, K.; Yu, J.; Li, B.-G.; Li, B.-F.; Pan, Z.-R. Chem Eng J 2000, 78, 211–215.
37. Paine, A. J. Macromolecules 1990, 23, 3109–3117.
38. Paine, A. J. J Colloid Interface Sci 1990, 138, 157–169.

Role of Dispersion Stabilizer with Hydroxy Groups in Preparation of Monodisperse Polylactide Microspheres

MAKOTO MURANAKA, TSUTOMU ONO

Department of Material and Energy Science, Graduate School of Environmental Science, Okayama University, 3-1-1 Tsushima-Naka, Okayama 700-8530, Japan

Received 27 December 2008; accepted 10 June 2009
DOI: 10.1002/pola.23572
Published online in Wiley InterScience (www.interscience.wiley.com).

ABSTRACT: Monodisperse poly(D,L-lactide) (PDLLA) microspheres were prepared by dispersion polymerization of D,L-lactide in xylene/heptane (1/2, *v/v*) with poly[(dodecyl methacrylate)-*co*-(2-hydroxyethyl methacrylate)] (P(DMA-*co*-HEMA)) as a dispersion stabilizer. P(DMA-*co*-HEMA) contains hydroxy groups, which act as an initiation group for pseudoanionic dispersion polymerization. The best coefficient of variation (CV) values concerning particle diameter distribution and the particle diameter of obtained PDLLA microspheres were 3.7% and 5.3 μm, respectively. The particle diameter decreased with increasing concentration of P(DMA-*co*-HEMA) and HEMA maintained low CV (<10%) values. As a result, monodisperse PDLLA microspheres ranging from 1.3 to 5.3 μm were obtained. In addition, it was found that monodisperse PDLLA microspheres were obtained by sufficient capture of growing polymers and monomers in the particle growth stage. Therefore, the HEMA concentration in P(DMA-*co*-HEMA) strongly affecting the capturing capability is the most important factor. © 2009 Wiley Periodicals, Inc. J Polym Sci Part A: Polym Chem 47: 5230–5240, 2009
Keywords: colloids; dispersion polymerization; micelles; monodisperse polylactide microspheres; stabilization

INTRODUCTION

Heterogeneous polymerization for preparing polymeric particles is mainly classified as emulsion,[1] dispersion,[2] and suspension polymerization.[3] Dispersion polymerization, which facilitates the preparation of microparticles with narrow diameter distribution in a single step, has attracted attention for biomedical and chemical applications such as coatings, inks, adhesives, and diagnosis carriers.[4–6] The degree of success in each application depends on the particle diameter and diameter distribution. Therefore, it is important to understand the role of the dispersion stabilizer and how to control the particle diameter and diameter distribution using the dispersion stabilizer.

Dispersion polymerization is carried out in a reaction medium that dissolves monomers, but not polymers. Polymerization continues in the reaction medium until the critical molecular weight of a polymer chain for solubility is reached, and then the precipitated particles are stabilized using the dispersion stabilizer. When using polystyrene-*b*-poly(ethylene glycol), which contains both soluble and insoluble polymer segments in a medium, as a dispersion stabilizer, Winnik and coworkers showed the existence of micelles comprised of several hundred molecules of a diblock copolymer and micellar clusters corresponding to the aggregation of tens of micelles in aqueous solution from dynamic light scattering measurements.[7,8] Moreover, in free radical polymerization,

Correspondence to: T. Ono (E-mail: tono@cc.okayama-u.ac.jp)
Journal of Polymer Science: Part A: Polymer Chemistry, Vol. 47, 5230–5240 (2009)

as the dissociation of an initiator is relatively slow, the duration of chain initiation is prolonged. Thus, the particle formation period in free radical dispersion polymerization with a diblock copolymeric stabilizer is complex. In contrast, *in-situ* polymerized graft copolymers are used during dispersion polymerization of styrene.[9–11] There are precursor polymers that contain active sites for chain transfer of radicals such as hydroxypropyl cellulose, poly(acrylic acid), and polyvinylpyrrolidone (PVP). As micelle formation of these polymeric stabilizers is negligible at the initial stage of polymerization, it would be promising to prepare monodisperse polystyrene microspheres. In a previous study, El-Aasser and coworkers prepared polystyrene microspheres with narrow diameter distribution by anionic dispersion polymerization using polystyrene-*b*-polybutadiene and *sec*-butyllithium as a dispersion stabilizer and an initiator, respectively.[12] During this anionic dispersion polymerization, all initiator was consumed by 1–2% of monomer.[13] Therefore, it is a favorable condition for understanding the role of the dispersion stabilizer.

Biodegradable polymeric microspheres have been recently developed for chemical materials such as coatings, inks, adhesives, and controlled drug delivery systems.[14–17] A typical biodegradable polymer, polylactide (PLA), exhibits good mechanical properties, biodegradability, and biocompatibility for use in those areas.[18–20] Slomkowski and coworkers reported that PLA microspheres with narrow diameter distribution, and a coefficient of variation (CV) of 12%, were prepared by dispersion polymerization of lactide in 1,4-dioxane/heptane (1:4, *v/v*) using poly(dodecyl acrylate)-*g*-poly(ε-caprolactone) as a dispersion stabilizer.[21–23] We also reported that poly(D,L-lactide) (PDLLA) microspheres with narrow diameter distribution and a CV of 12.5%, were prepared by dispersion polymerization of D,L-lactide in xylene/heptane (1:2, *v/v*) using copolymer grafting PLLA, poly(dodecyl methacrylate)-*g*-polylactide, as a dispersion stabilizer.[24,25] However, monodisperse PDLLA microspheres with a CV < 10%, have not been obtained.

We have synthesized poly[(dodecyl methacrylate)-*co*-(2-hydroxyethyl methacrylate)] (P(DMA-*co*-HEMA)) containing hydroxy groups, which act as an initiation group for pseudoanionic dispersion polymerization, leading to the formation of the PDLLA-grafted copolymer, P(DMA-*co*-HEMA)-*g*-PDLLA. Consequently, P(DMA-*co*-HEMA) brought about monodisperse PDLLA microspheres by pseudoanionic dispersion polymerization of D,L-lactide.[26] The advantage of P(DMA-*co*-HEMA) was the formation of a graft copolymer *in situ*. Omi et al. reported that the addition of a small amount of L-ascorbic acid (AA) provided monodisperse polystyrene microspheres during dispersion polymerization with PVP as a dispersion stabilizer.[27] AA acted as an antioxidant, and the oxidized form of AA takes part in the abstraction of a hydrogen atoms from PVP. As a result, monodisperse polystryrene microspheres were prepared by promoting the grafting of PVP. Therefore, the grafting of a dispersion stabilizer produced *in situ* is the most important factor in preparing monodisperse polymeric microspheres by dispersion polymerization. P(DMA-*co*-HEMA) contains initiation points of polymerization, and the number of points are controllable. Therefore, we expect there exists an optimal graft chain number in a grafted copolymeric stabilizer for preparing monodisperse PDLLA microspheres. We investigated the role of P(DMA-*co*-HEMA) in the control of particle diameter and diameter distribution during dispersion polymerization and suggested a solution for preparing monodisperse PDLLA microspheres.

EXPERIMENTAL

Materials

D,L-Lactide (Purac) was purified by recrystallization from toluene. 2-Hydroxyethyl methacrylate (HEMA), dodecyl methacrylate (DMA) (Wako Pure Chemical Industries, Ltd.), and tin(II) 2-ethylhexanoate (Aldrich) were purified by distillation under reduced pressure.[28,29] Xylene and heptane (dehydrated-grade) (Wako Pure Chemical Industries, Ltd.) were stored in a glove box filled with argon gas. Other reagents (Wako Pure Chemical Industries, Ltd.) were used as received.

P(DMA-*co*-HEMA) Synthesis

The synthesis of P(DMA-*co*-HEMA), C_2 in Table 1, is described as a typical example of synthesis. DMA (7.9 g, 31.18 mmol), HEMA (81 mg, 0.62 mmol), and dehydrated toluene (24 mL) were placed into a round-bottom reactor. After nitrogen was added to remove oxygen, the reactor was immersed in an oil bath at 358 K. Dehydrated toluene dissolved in benzoyl peroxide (BPO) (304 mg, 1.25 mmol) was added to initiate polymerization. Polymerization was conducted for 3 h.

Table 1. Molecular Structure of P(DMA-*co*-HEMA)

Code	M_n	M_w/M_n	F_{HEMA} (mol %)	N_{HEMA} (units)
H_1	8,200	2.16	0.0	0.0
C_1	16,900	2.42	0.9	0.6
C_2	16,300	2.48	1.3	0.8
C_3	18,200	2.44	2.3	1.7
C_4	17,000	2.24	4.1	2.9

Afterward, the reaction mixture was poured into excess methanol to remove the remaining DMA and HEMA. After purification, the obtained polymer was dried under reduced pressure at 313 K.

PDLLA Microspheres Preparation

PDLLA microspheres were prepared according to a typical preparation procedure of PDLLA microspheres shown in Scheme 1. D,L-lactide (500 mg, 3.47 mmol) was added into dehydrated xylene/heptane (1:2, *v/v*) (17 mL) dissolved in P(DMA-*co*-HEMA). The solution was stirred at 120 rpm with a magnetic stirrer. Dehydrated xylene/heptane (1:2, *v/v*) (3 mL) dissolved in stannous 2-ethylhexanoate (475 mg, 0.12 mmol) as a catalyst was prepared. This was added into the solution using a syringe, and polymerization was conducted at 368 K for 3 h. After polymerization, the reaction solution was poured into excess cold heptane. The solution was centrifuged for 3 min at 6000 rpm, and the collected microspheres were redispersed into heptane. This solution was filtered to collect the prepared microspheres. During polymerization, aliquots of the sample were periodically withdrawn through a syringe for intermittent characterization of the polymerization progress.

Characterization

The chemical structures of the synthesized polymers were confirmed with ^1H NMR (AL300 SC-NMR, JEOL) using $CDCl_3$ as a solvent. The weight-averaged molecular weight (M_w) and the polydispersity index (M_w/M_n) of the synthesized polymers were measured using gel permeation chromatography (HLC 8120, Tosoh, GPC) equipped with a refractive index detector based on polystyrene standards with tetrahydrofuran as an eluent. A scanning electron microscope (S-4700, Hitachi, SEM) was used to study the morphology of PDLLA microsphers, particle diameter, and diameter distribution. Dynamic light scattering measurement (FPAR-1000, Otsuka Electronics Co., DLS) was carried out at 293 K using a He-Ne laser with a wavelength of 633 nm to determine the hydrodynamic diameter (R_h) of the micelles of P(DMA-*co*-HEMA) and P(DMA-*co*-HEMA)-*g*-PDLLA in xylene/heptane (1:2, *v/v*). The mean hydrodynamic diameter was evaluated using the cumulant method. The conversion of D,L-lactide was measured using high-performance liquid chromatography (LC-6A, Shimazu, HPLC) with methanol/water (1:49, *v/v*) as an eluent and a UV-detector at 216 nm.

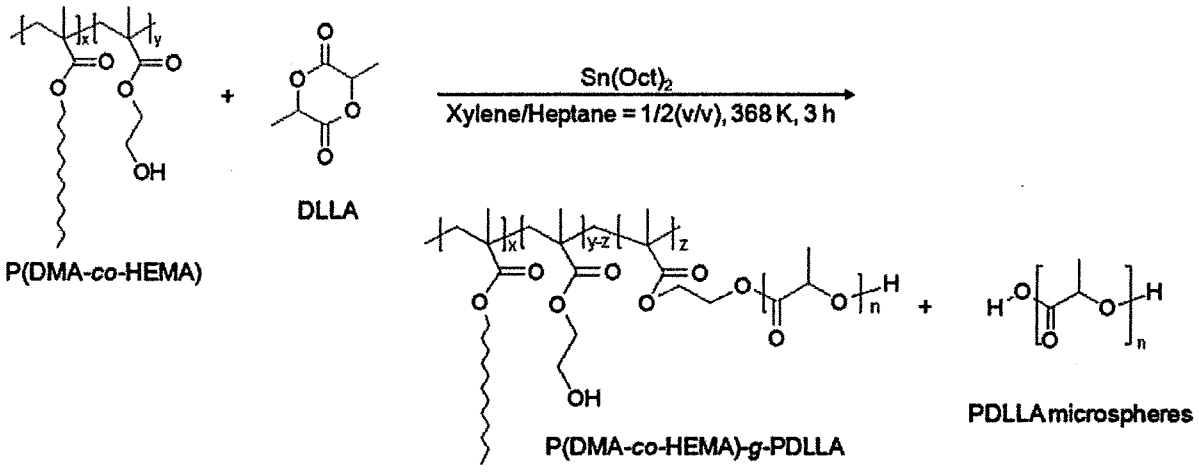

Scheme 1. Preparation of PDLLA microspheres.

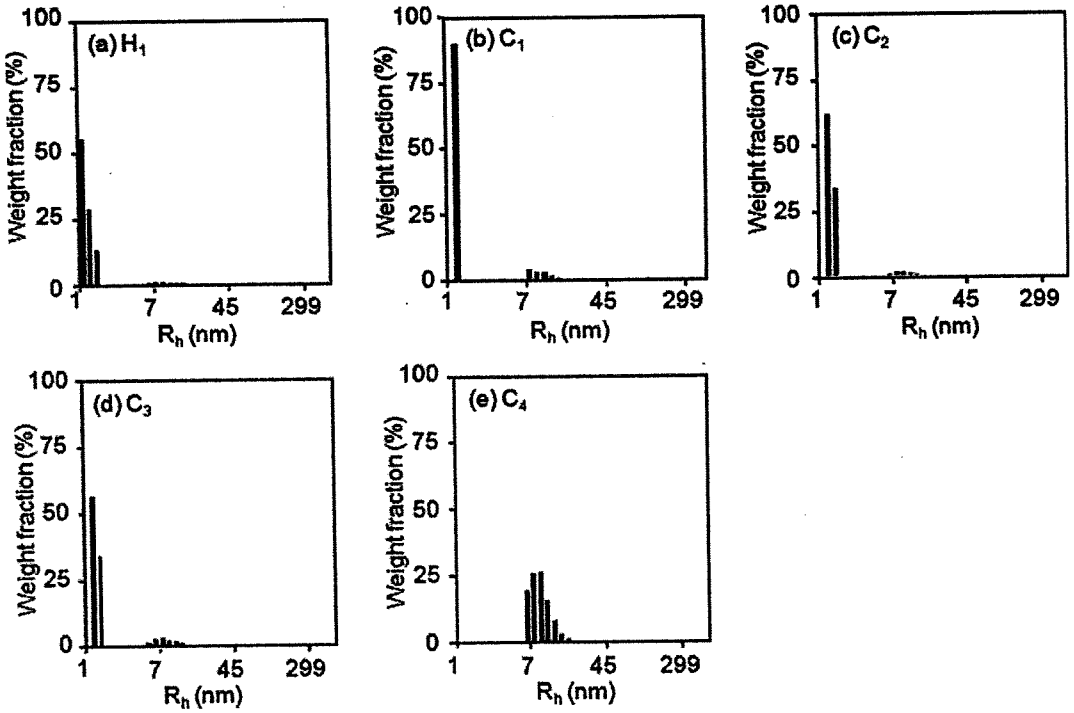

Figure 1. Size distributions of P(DMA-*co*-HEMA) in xylene/heptane (1:2, *v/v*); (a) H_1 (R_h = 1.1 and 8.6 nm), (b) C_1 (R_h = 1.2 and 8.6 nm), (c) C_2 (R_h = 1.3 and 8.8 nm), (d) C_3 (R_h = 1.3 and 7.4 nm), and (e) C_4 (R_h = 7.9 nm), [P(DMA-*co*-HEMA)] = 10 g/L.

RESULTS AND DISCUSSION

P(DMA-*co*-HEMA) Synthesis

P(DMA-*co*-HEMA) was successfully obtained by free radical copolymerization of DMA and HEMA using BPO as an initiator. The analytical results of synthesized copolymers are summarized in Table 1. To investigate the effect of the molecular structure of P(DMA-*co*-HEMA) on the particle diameter and diameter distribution of PDLLA microspheres, five kinds of P(DMA-*co*-HEMA) with different HEMA concentrations were synthesized. The ^{1}H NMR spectrum of P(DMA-*co*-HEMA) showed peaks at 3.9 ppm ($COOCH_2$ for DMA unit) and at 4.1 ppm ($COOCH_2$ for HEMA unit). Furthermore, there were no peaks detected around 5.6 and 6.1 ppm (double bond for DMA and HEMA) in the spectrum. Therefore, P(DMA-*co*-HEMA) was finally identified. The fraction of HEMA units in P(DMA-*co*-HEMA), F_{HEMA}, was calculated by the integration ratios corresponding to 3.9 ppm ($COOCH_2$ for DMA unit) and 4.1 ppm ($COOCH_2$ for HEMA unit) in the ^{1}H NMR spectrum.

This was defined by the following equation:

$$F_{HEMA} = \frac{A_{HEMA}}{(A_{DMA} + A_{HEMA})}$$

where A_{HEMA} and A_{DMA} denote the peak areas of $COOCH_2$ for HEMA and DMA units in the ^{1}H NMR spectrum of P(DMA-*co*-HEMA), respectively. The number of HEMA units in P(DMA-*co*-HEMA), N_{HEMA}, is defined as follows:

$$N_{HEMA} = \frac{M_{n\ copolymer}}{(M_{n\ DMA}\frac{A_{DMA}}{A_{HEMA}} + M_{n\ HEMA})}$$

where $M_{n\ copolymer}$, $M_{n\ DMA}$, and $M_{n\ HEMA}$ denote the number-averaged molecular weight of P(DMA-*co*-HEMA), DMA, and HEMA, respectively.

DLS Measurement of P(DMA-*co*-HEMA)

DLS measurements clarified the presence of P(DMA-*co*-HEMA) micelles, as shown in Figure 1. P(DMA-*co*-HEMA) exhibited a bimodal size distribution based on unimers and polymeric micelles

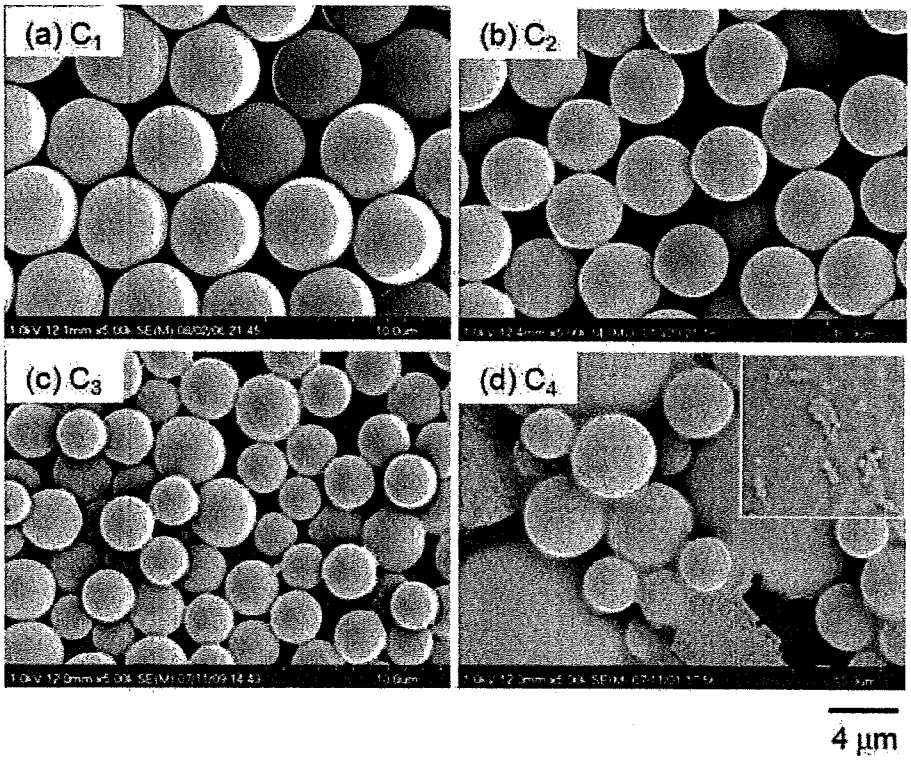

Figure 2. SEM images of PDLLA microspheres prepared by dispersion polymerization using P(DMA-*co*-HEMA) with different HEMA concentrations; (a) C_1 (dp = 5.3 μm, CV = 3.7%), (b) C_2 (dp = 4.5 μm, CV = 4.9%), (c) C_3 (dp = 3.2 μm, CV = 13%), and (d) C_4 (polydispersity), [P(DMA-*co*-HEMA)] = 1.0 g/L.

in xylene/heptane (1:2, *v/v*) when using H_1, C_1, C_2, and C_3 (refer Table 1). The mean hydrodynamic diameter (R_h) of unimers and polymeric micelles were about 1.3 and 8.0 nm, respectively. In addition, most of the P(DMA-*co*-HEMA) were in a unimer state in the solution. In contrast, when using C_4, P(DMA-*co*-HEMA) exhibited a single size distribution based on the polymeric micelles in the solution. This result indicated that the formation of polymeric micelles was induced by the existence of hydroxy groups in P(DMA-*co*-HEMA), which showed a low affinity to the medium. Winnik and coworkers reported that the large molecular weight block copolymers showed the presence of micellar aggregates in methanol, which might induce the polydispersity of the particles during dispersion polymerization.[8] Therefore, it was assumed that the HEMA concentration in P(DMA-*co*-HEMA) affecting micelle formation should be a contributing factor to prepare monodisperse PDLLA microspheres during dispersion polymerization of D,L-lactide.

Effect of HEMA Concentration on Particle Size Distribution

Figure 2 shows SEM images of PDLLA microspheres prepared by dispersion polymerization using P(DMA-*co*-HEMA) with different HEMA concentrations. As shown in Figure 2, monodisperse PDLLA microspheres were obtained using only C_1 and C_2. The best value of CV and the particle diameter of PDLLA microspheres were 3.7% and 5.3 μm, respectively [Fig. 2(a)]. In contrast, PDLLA microspheres were not obtained during dispersion polymerization using H_1, which had no HEMA unit. These results suggested that the preparation of spherical PDLLA microspheres require a dispersion stabilizer containing PDLLA segments to interact with the precipitated particles. The PDLLA segment in a dispersion stabilizer physically adsorbs on the surface of the precipitated particles, and the PDMA segment creates high solubility in the medium. In addition, the CV increased with increasing HEMA concentrations in P(DMA-*co*-HEMA), and polydisperse

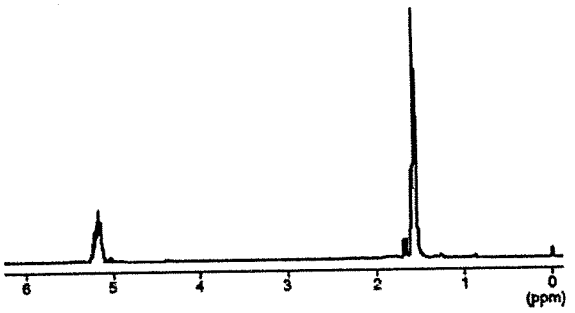

Figure 3. ^{1}H NMR spectrum of PDLLA microspheres prepared by dispersion polymerization using P(DMA-*co*-HEMA) (C_2).

PDLLA microspheres were prepared during dispersion polymerization using C_3 and C_4 [Fig. 2(c,d)]. In particular, many nanoparticles of P(DMA-*co*-HEMA)-*g*-PDLLA were obtained when using C_4 because most monomers were consumed by the hydroxy groups in P(DMA-*co*-HEMA) during polymerization. Therefore, we concluded that there is an optimal HEMA concentration for preparing monodisperse PDLLA microspheres.

Characterization of PDLLA Microspheres

Figure 3 shows the ^{1}H NMR spectrum of PDLLA microspheres prepared by dispersion polymerization using C_2 as a dispersion stabilizer. The spectrum showed peaks at 1.7 and 5.2 ppm (CH_3 and CH for PLA), but no peaks of P(DMA-*co*-HEMA)-*g*-PDLLA were detected. During dispersion polymerization of styrene or methyl methacrylate using a conventional stabilizer, PVP and the existence of a graft copolymer on the surface of particles were confirmed using FTIR and X-ray photoelectron spectroscopy.[30,31] This suggests that the adsorption of P(DMA-*co*-HEMA)-*g*-PDLLA on the particle surface was weak. In addition, no peak at 4.1 ppm ($COOCH_2$ for HEMA unit) was detected in the ^{1}H NMR spectrum of P(DMA-*co*-HEMA)-*g*-PDLLA. Therefore, all hydroxy groups in P(DMA-*co*-HEMA)reacted, and PDMA-*g*-PDLLA was produced *in situ*. The number-averaged molecular weight of the graft chain was approx. 14,000. Furthermore, Figure 4 shows the size distribution of PDMA-*g*-PDLLA in the supernatant of the medium after dispersion polymerization. The resultant graft copolymer, PDMA-*g*-PDLLA, exhibited a single size distribution based on the polymeric micelles through self-aggregation. Consequently, it was confirmed that

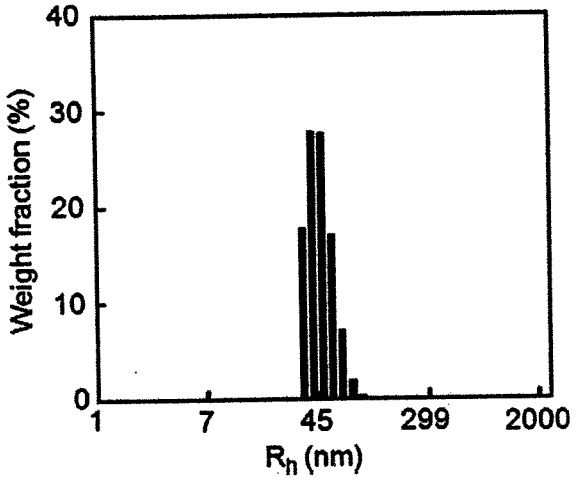

Figure 4. Size distribution of P(DMA-*co*-HEMA)-*g*-PDLLA in supernatant of medium after dispersion polymerization; [P(DMA-*co*-HEMA) (C_2)] = 1.0 g/L.

hydroxy groups in P(DMA-*co*-HEMA) played a key role as an initiation group during polymerization of D,L-lactide.

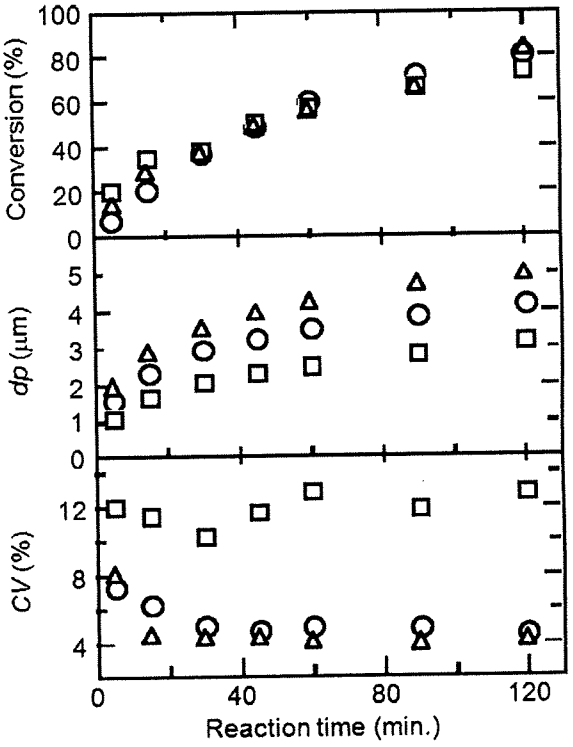

Figure 5. Dependence of monomer conversion, particle diameter, and diameter distribution of PDLLA microspheres on polymerization times, P(DMA-*co*-HEMA); C_1 (△), C_2 (○), C_3 (□), [P(DMA-*co*-HEMA)] = 1.0 g/L.

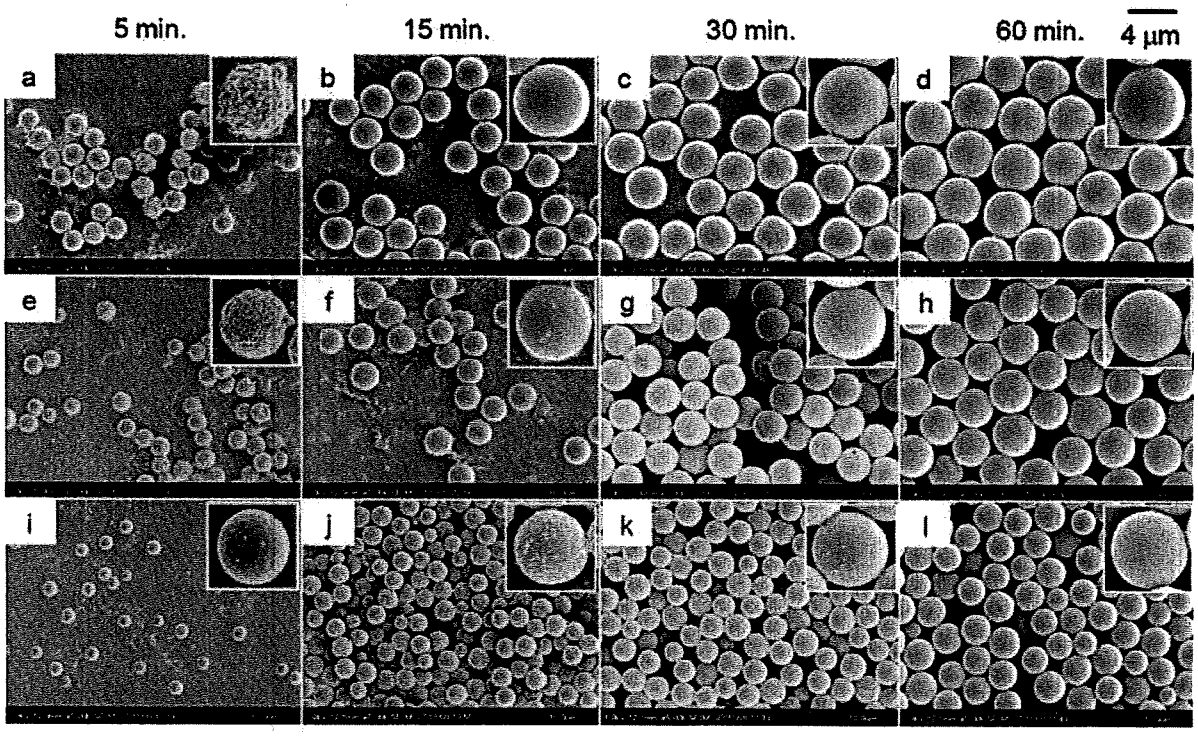

Figure 6. SEM images of PDLLA microspheres at 5, 15, 30, and 60 min of dispersion polymerization using P(DMA-*co*-HEMA) with different HEMA concentrations; (a–d) C_1, (e–h) C_2, (i–l) C_3, [P(DMA-*co*-HEMA)] = 1.0 g/L.

Time Courses of Particle Growth

The effects of polymerization time on monomer conversion, the particle diameter and particle diameter distribution on HEMA concentration in P(DMA-*co*-HEMA) were investigated for preparing monodisperse PDLLA microspheres. The results are shown in Figure 5. From Figure 5, the CV decreased with increasing polymerization time when using C_1 and C_2. The decrease in CV was induced by the capture of growing polymers and monomers into the particles from a continuous phase in the particle growth stage.[32,33] In contrast, CV did not decrease with increasing polymerization time when using C_3. In soap-free polymerization, Yamamoto et al. reported that the rough surface of polystyrene latex particles became smooth by the addition of styrene monomers in the particle growth stage.[34,35] We observed the surface morphology of the particles, which changed with increasing polymerization time, using SEM as well as these reports. Figure 6 shows SEM images of PDLLA microspheres at 5, 15, 30, and 60 min of dispersion polymerization using P(DMA-*co*-HEMA) with different HEMA concentrations. C_1 exhibited the roughest particle surface at 5 min, becoming smooth at 15 min. In contrast, the surface became smooth at 60 min with C_3. These results suggest that the growing polymers and monomers were not sufficiently captured into the particles in the particle growth stage because many monomers were consumed by the hydroxy groups in P(DMA-*co*-HEMA) during polymerization. Therefore, with C_3, the CV did not decrease due to insufficient capture of growing polymers and monomers. With C_1 and C_2, monodisperse PDLLA microspheres were obtained by sufficient capture of growing polymers and monomers. In conclusion, the HEMA concentrations in P(DMA-*co*-HEMA) strongly affected the capability of capturing monomers and growing polymers, and P(DMA-*co*-HEMA) with 0.9 mol % of HEMA was the optimal molecular structure.

Effect of P(DMA-*co*-HEMA) Concentration

P(DMA-*co*-HEMA), a dispersion stabilizer, plays an important role in preparing monodisperse PDLLA microspheres during dispersion polymer-

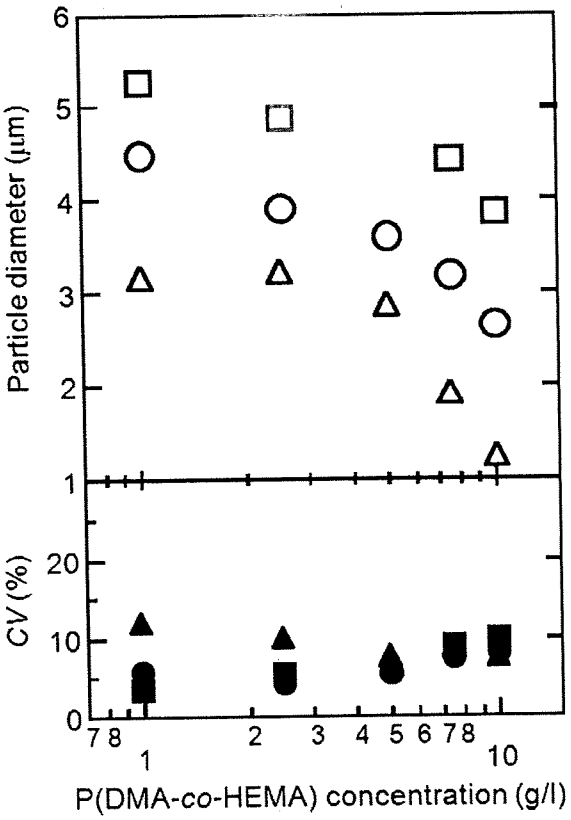

Figure 7. Effect of P(DMA-*co*-HEMA) concentration on particle diameter and diameter distribution of PDLLA microspheres; C_1 (□, ■), C_2 (○, ●), C_3 (△, ▲).

ization. P(DMA-*co*-HEMA) and P(DMA-*co*-HEMA)-*g*-PDLLA adsorb onto the surface of particles through physical interaction. In fact, *in-situ* produced P(DMA-*co*-HEMA)-*g*-PDLLA acts as a true dispersion stabilizer to form spherical stable particles and inhibits particle coagulation. Figure 7 shows the effect of P(DMA-*co*-HEMA) concentration on the particle diameter and diameter distribution of PDLLA microspheres prepared using P(DMA-*co*-HEMA) with different HEMA concentrations. From Figure 7, the particle diameter decreased with increasing P(DMA-*co*-HEMA) concentration because a large number of P(DMA-*co*-HEMA) molecules adsorbed onto the large surface area of particles to reduce the surface energy. In addition, the particle diameter decreased with increasing HEMA concentration in P(DMA-*co*-HEMA) because the adsorption rate to the surface of particles was larger when using P(DMA-*co*-HEMA) with a number of PDLLA chains, which showed a high affinity to the particles. In conclusion, the particle diameters of monodisperse PDLLA microspheres were controlled from 1.3 to 5.3 μm by the P(DMA-*co*-HEMA) and HEMA concentrations. Figure 8 shows the largest and smallest monodisperse PDLLA microspheres obtained in this study.

The CV increased with increasing P(DMA-*co*-HEMA) concentration when using C_1 and C_2. The decrease in CV was induced by the capture of growing chains and monomers into the particles

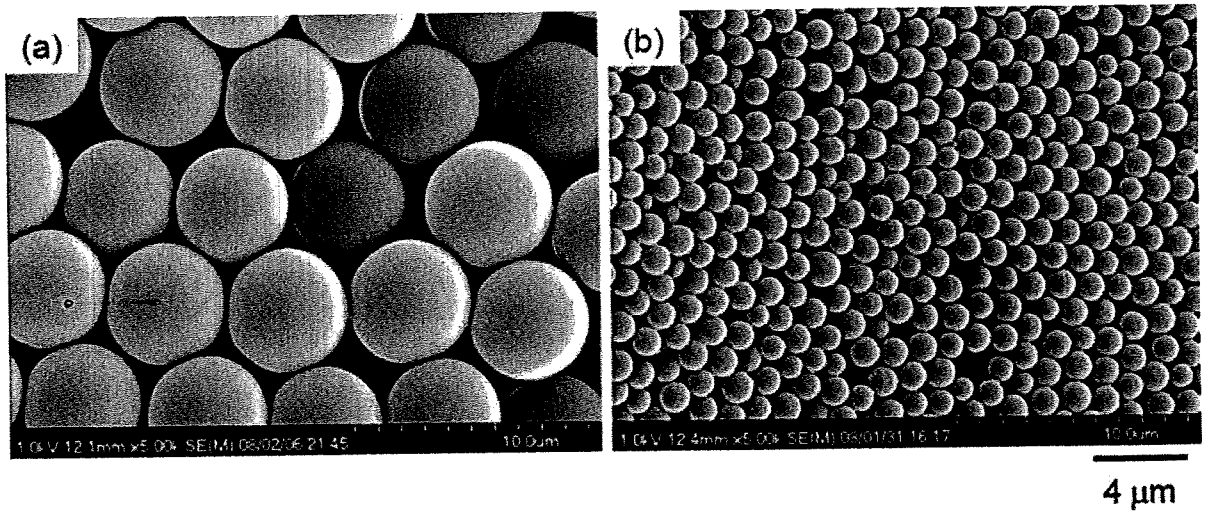

Figure 8. SEM images of PDLLA microspheres prepared with different concentrations of P(DMA-*co*-HEMA); (a) [C_1] = 1.0 g/L (dp = 5.3 μm, CV = 3.7%), (b) [C_3] = 10 g/L (dp = 1.3 μm, CV = 7.7%).

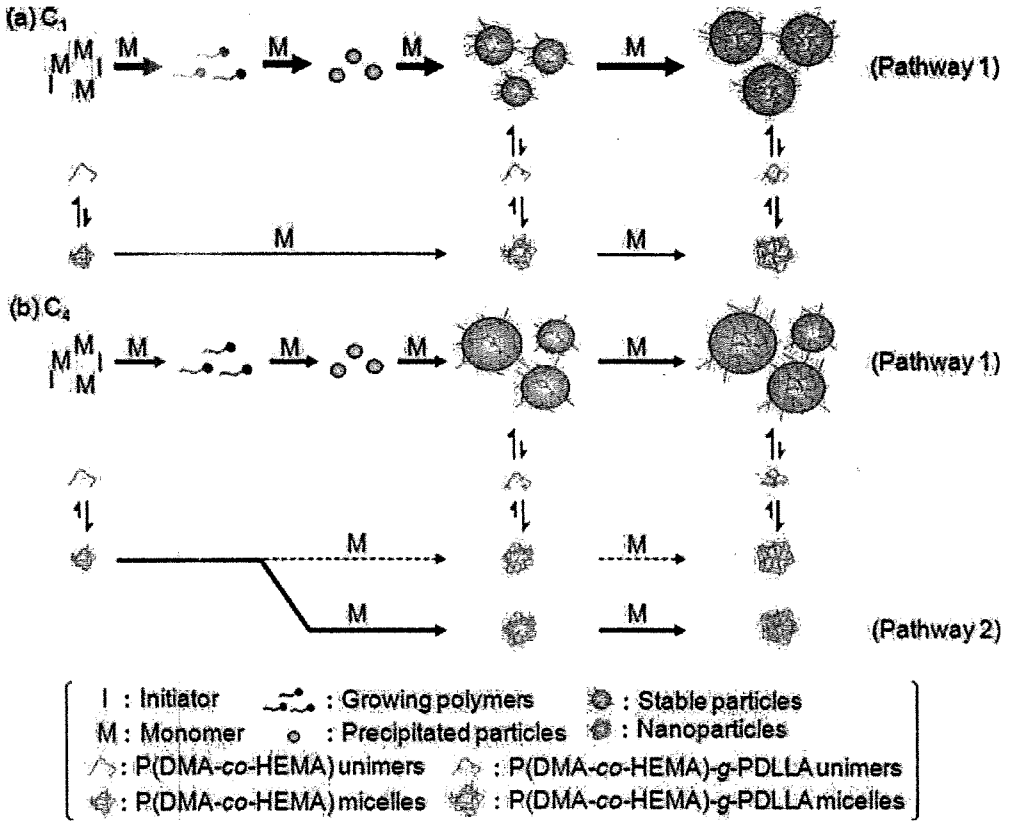

Figure 9. Schematic representation of particle formation and growth during dispersion polymerization of D,L-lactide with P(DMA-*co*-HEMA), (a) C_1, (b) C_4, [P(DMA-*co*-HEMA)] = 1.0 g/L.

from a continuous phase in the particle growth stage. Therefore, with increasing P(DMA-*co*-HEMA) concentration, captured monomers in the particles decreased due to the fact that many monomers were consumed by polymerization from the hydroxy groups in P(DMA-*co*-HEMA). On the other hand, with C_3, the CV decreased with increasing P(DMA-*co*-HEMA) concentration. This result indicated that more monomers were consumed by the hydroxy groups in P(DMA-*co*-HEMA) during polymerization because C_3 had more hydroxy groups, and hence P(DMA-*co*-HEMA)-*g*-PDLLA quickly formed at the initial stage. As a result, the anchoring of P(DMA-*co*-HEMA)-*g*-PDLLA onto the precipitated particles inhibited coagulation of precipitated particles at the stable particle formation stage.

Formation Mechanism of Particles

In general, regardless of the molecular structures of the dispersion stabilizer, the formation mechanism of particles for dispersion polymerization is basically the same as the one we proposed.[36,37] Based on the results in the above sections and the proposed mechanism earlier in the literature for dispersion polymerization of lactide, the formation mechanism of particles during dispersion polymerization of D,L-lactide in xylene/heptane (1:2, *v/v*) using P(DMA-*co*-HEMA) with different HEMA concentrations is illustrated in Figure 9. C_1, C_2, and C_3 with <2.30 mol % of HEMA exhibited a unimer state in the medium. Therefore, polymerization occurs in a homogeneous medium, and then the generated polymer chains grow until reaching the critical chain length where they precipitate to form particles. These precipitated particles are unstable and easily aggregate with each other. Simultaneously, the graft copolymeric stabilizer produced *in situ*, P(DMA-*co*-HEMA)-*g*-PDLLA, adsorbs on the aggregates of the precipitated particles, forming stable particles. The stable particles grow by capturing monomers and growing polymers into the particles from a

continuous phase, which results in PDLLA microspheres (Pathway 1). In particular, monodisperse PDLLA microspheres are obtained by the sufficient capture of growing polymers and monomers into the particles from a continuous phase in the particle growth stage when using C_1 with the lowest HEMA concentration [Fig. 9(a)]. Moreover, nanoparticles of P(DMA-*co*-HEMA)-*g*-PDLLA are formed when using C_4 with the highest HEMA concentration because most monomers are consumed by the hydroxy groups in P(DMA-*co*-HEMA) during polymerization (Pathway 2). As a result, the number of P(DMA-*co*-HEMA)-*g*-PDLLA, which stabilizes PDLLA microspheres in pathway 1, decreases, and polydisperse and larger PDLLA microspheres are obtained [Fig. 9(b)].

CONCLUSIONS

We developed monodisperse PDLLA microspheres by dispersion polymerization in xylene/heptane (1/2, *v/v*) using P(DMA-*co*-HEMA) as a dispersion stabilizer containing hydroxy groups. When using P(DMA-*co*-HEMA) with 0.9 mol % of HEMA, the best result in the CV of PDLLA microspheres obtained in this study was 3.7%, and the particle diameter was 5.3 μm. In addition, by keeping CV low (<10%), the particle diameter was controllable from 1.3 to 5.3 μm by altering the concentrations of P(DMA-*co*-HEMA) and HEMA, which affect the adsorption of *in-situ* polymerized P(DMA-*co*-HEMA)-*g*-PDLLA onto the precipitated particles until stable particles are formed. When monodisperse PDLLA microspheres were obtained, the CV decreased with increasing polymerization time by the sufficient capturing of growing polymers and monomers into the particles from a continuous phase in the particle growth stage. The capturing depended on the consumption of monomer by polymerization from hydroxy groups in P(DMA-*co*-HEMA). Therefore, the HEMA concentration in P(DMA-*co*-HEMA) strongly affected the capturing capability, which was the most important factor. Consequently, preparation of modisperse PDLLA microspheres and the particle diameter control were attain using a new molecular design of a dispersion stabilizer.

REFERENCES AND NOTES

1. Smith, W. V. J Am Chem Soc 1948, 70, 3695–3702.
2. Barrett, K. E. J.; Thomas, H. R. J Polym Sci Part A: Polym Chem 1969, 7, 2621–2650.
3. Bergquist, N. R.; Holubar, K.; Diaz, G. A.; Beutner, E. H. Int Arch Allergy Appl Immunol 1972, 43, 791–799.
4. Van Den Hul, H. J.; Vanderhoff, J. W. J Colloid Interface Sci 1968, 28, 336–337.
5. Paine, A. J. J Colloid Interface Sci 1990, 138, 157–169.
6. Okubo, M.; Kondo, Y.; Takahashi, M. Colloid Polym Sci 1993, 271, 109–113.
7. Xu, R.; Winnik, M. A.; Hallett, F. R.; Riess, G.; Croucher, M. D. Macromolecules 1991, 24, 87–93.
8. Winzor, C. L.; Mrazek, Z.; Winnik, M. A.; Croucher, M. D.; Riess, G. Eur Polym J 1994, 30, 121–128.
9. Ober, C. K.; Lok, K. P. Macromolecules 1987, 20, 268–273.
10. Lu, Y. Y.; El-Aasser, M. S.; Vanderhoff, J. W. J Polym Sci Part B: Polym Phys 1988, 26, 1187–1203.
11. Tseng, C. M.; Lu, Y. Y.; El-Assser, M. S.; Vanderhoff, J. W. J Polym Sci Part A: Polym Chem 1986, 24, 2995–3007.
12. Awan, M. A.; Dimonie, V. L.; El-Aasser, M. S. J Polym Sci Part A: Polym Chem 1996, 34, 2633–2649.
13. Hsieh, H. L. J Polym Sci Part A: Polym Chem 1965, 3, 163–172.
14. Doi, Y. Kobunshi Ronbunshu 2006, 63, 86–97.
15. Sawalha, H.; Purwanti, N.; Rinzema, A.; Schroen, K.; Boom, R. J Membr Sci 2008, 310, 484–493.
16. Matsuyama, K.; Donghui, Z.; Urabe, T.; Mishima, K. J Supercrit Fluids 2005, 33, 275–281.
17. Ouchi, T.; Hamada, A.; Ohya, Y. Macromol Chem Phys 1999, 200, 436–441.
18. Eling, B.; Gogolewski, G.; Pennings, A. J. Polymer 1982, 23, 1587–1593.
19. Leenslag, J. W.; Pennings, A. J. Polymer 1987, 28, 1695–1702.
20. Macdonald, R. T.; Mccarthy, S. P.; Gross, R. A. Macromolecules 1996, 29, 7356–7361.
21. Sosnowski, S.; Gadzinowski, M.; Slomkowski, S.; Penczek, S. J Bioact Compat Polym 1994, 9, 345–366.
22. Sosnowski, S.; Gadzinowski, M.; Slomkowski, S. Macromolecules 1996, 29, 4556–4564.
23. Slomkowski, S.; Sosnowski, S.; Gadzinowski, M. Colloids Surf A 1999, 153, 111–118.
24. Muranaka, M.; Kitamura, Y.; Yoshizawa, H. Colloid Polym Sci 2007, 285, 1441–1448.
25. Muranaka, M.; Yoshizawa, H.; Ono, T. Colloid Polym Sci 2009, 287, 525–532.
26. Muranaka, M.; Ono, T. Macromol Rapid Commun 2009, 30, 152–156.
27. Omi, S.; Saito, M.; Hashimoto, T.; Nagai, M.; Ma, G. J Appl Polym Sci 1998, 68, 897–907.
28. Raghunadh, V.; Baskaran, D.; Sivaram, S. Polymer 2004, 45, 3149–3155.
29. Kowalski, A.; Duda, A.; Penczek, S. Macromol Rapid Commun 1998, 19, 567–572.

Journal of Polymer Science: Part A: Polymer Chemistry
DOI 10.1002/pola

30. Shen, S.; Sudol, E. D.; El-Aasser, M. S. J Polym Sci Part A: Polym Chem 1994, 32, 1087–1100.
31. Bamnolker, H.; Margel, S. J Polym Sci Part A: Polym Chem 1996, 34, 1857–1871.
32. Paine, A. J. Macromolecules 1990, 23, 3109–3117.
33. Araujo, P. H. H.; Pinto, J. C. Braz J Chem Eng 2000, 17, 383–394.
34. Yamamoto, T.; Fukushima, T.; Kanda, Y.; Higashitani, K. J Colloid Interface Sci 2005, 292, 392–396.
35. Yamamoto, T.; Nakayama, M.; Kanda, Y.; Higashitani, K. J Colloid Interface Sci 2006, 297, 112–121.
36. Sosnowski, S.; Slomkowski, S.; Lorenc, A.; Krichel-dorf, H. R. Colloid Polym Sci 2002, 280, 107–115.
37. Slomkowski, S.; Sosnowski, S.; Gadzinowski, M. Polimery 2002, 47, 485–490.

LETTER

A Versatile Biodegradable Polymer with a Thermo-Reversible/Irreversible Transition

Fumiaki Tanimoto, Yoshiro Kitamura, Tsutomu Ono,* and Hidekazu Yoshizawa

Department of Material and Energy Science, Graduate School of Environmental Science, Okayama University

ABSTRACT A versatile biodegradable thermoresponsive polymer was developed. The polymer has succinimide and isopropylasparamide segments and exhibits a phase transition with thermoreversibility that can be controlled by changing the polymer composition. With fewer succinimide units, the polymer exhibits the type of thermo-reversible phase transition that is characteristic of poly(*N*-isopropylacrylamide) (PNIPAAm). The polymer with a higher proportion of succinimide units exhibits a thermo-irreversible phase transition, resulting in the formation of nanospheres that are stable below the transition temperature. The stable nanospheres are generated by dehydration and subsequent conformational stabilization through an interaction between imide rings. This thermoirreversible phase transition in water provides a simple, oil-free preparation of biodegradable nanospheres.

KEYWORDS: thermoresponsive polymer • irreversible phase transition • poly(aspartic acid) • biodegradable nanosphere • poly(succinimide)

Stimuli-responsive polymers have many potential applications because their properties change dramatically in response to external stimuli such as temperature, pH, and electric field (1−4). Thermoresponsive polymers whose water solubility changes abruptly in response to temperature have been extensively investigated for use in practical applications such as drug delivery vehicles, bioseparation reagents, and surface modifiers, as well as for academic interest to elucidate mechanisms of heat denaturation of proteins (5−7). Attention has mostly been paid to thermoresponsive polymers with lower critical solution temperatures (LCST) in water (8−11). These polymers are water-soluble below the LCST because of their hydrated extended chain conformation, and lose their water solubility above the LCST because of their nonhydrated collapsed chain conformation (12). Although polymer materials are often required to be biodegradable to be useful in fields such as medicine, biology, and environmental science, conventional thermoresponsive polymers such as poly(*N*-isopropylacrylamide) (PNIPAAm) and its copolymers are not degradable. Here, we report a versatile biodegradable thermoresponsive polymer with regulatable thermoreversibility that can be controlled by changing its composition.

Poly(aspartic acid) synthesized by acid-catalyzed polycondensation of L-aspartic acid followed by alkaline hydrolysis is known to be biodegradable and water-soluble (13, 14). Aminolysis of an intermediate product, poly(succinimide) (PSI), with nucleophilic amino compounds is used to form various poly(asparamide)s with functional groups in side chains (15−19). To synthesize thermoresponsive poly(asparamide), we used isopropylamine, which gave a PNIPAAm-like side chain structure, because the thermoresponsivity of PNIPAAm is ascribed to its N-isopropylamide side chain structure. Poly[α,β-(DL-asparate isopropylamide)-*co*-(succinimide)] (designated IPA-PSI) was obtained (Scheme 1) by aminolysis of PSI with isopropylamine in dimethylformamide: the details of the synthesis are described in the Supporting Information. Because poly(aspartic acid)s with dodecyl groups in the side chains have showed biodegradability (16), poly(aspartate) was expected to be a biodegradable polymer. IPA-PSI was gradually converted into poly(aspartate) with thermoresponsive side chains by alkali hydrolysis; therefore IPA-PSI was also expected to be biodegradable.

The mole fraction of isopropylasparamide units in the polymer (hereafter referred to as the degree of substitution) was varied from 30 to 76 mol %. Complete aminolysis of succinimide with isopropylamine did not occur even at the highest mole ratio of isopropylamine to the succinimide unit of PSI in the feed. This might be due to the steric hindrance of the branched alkyl group of isopropylamine because the aminolysis reaction of PSI with propylamine, a nucleophile with a straight alkyl chain, proceeded almost to completion at the same mole ratio of propylamine to the succinimide unit of PSI. Aminolysis of one hydrophobic succinimide unit with one isopropylamine molecule produces one hydrophobic isopropyl group and two hydrophilic amide bonds, thus increasing the hydrophilicity of the polymer. Consequently, the degree of substitution (DS) has a significant effect on the water solubility of the synthesized IPA-PSI. The effect of DS on water solubility is illustrated in Figure 1a. PSI and IPA-PSI with DS < 30 mol % were consistently insoluble in ultra pure water (ultrafiltered with a Milli-Q water purification system) in the temperature range 0−100 °C, and their cloud points were not determined. IPA-PSI with DS > 37 mol %, on the other hand, dissolved freely in ultra pure water. The thermo-responsivity of water-soluble IPA-PSI was of two

* Corresponding author. Tel: +81-86-251-8908. Fax: +81-86-251-8908. E-mail: tono@cc.okayama-u.ac.jp.

Received for review October 17, 2009 and accepted February 16, 2010

DOI: 10.1021/am900705s

Scheme 1. Synthesis of IPA-PSI

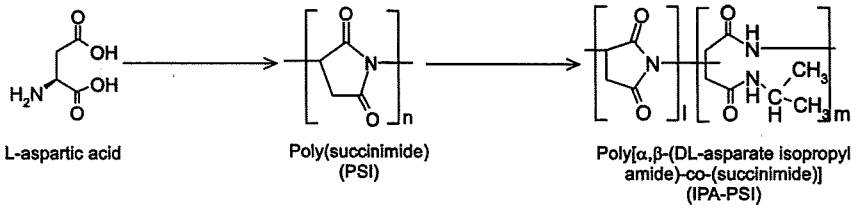

types, corresponding to reversible and irreversible phase transitions, according to the magnitude of DS (Figure 1a).

Aqueous solutions of IPA-PSI with DS > 37 mol % became turbid after being heated to above their cloud point, due to dehydration of the thermoresponsive isopropylamide units. A reversible phase transition was observed for aqueous solutions of IPA-PSIs with DS in the range 62–76 mol %, which were transparent after cooling, as for a conventional thermo-responsive polymer (Figure 1b). By contrast, aqueous solutions of IPA-PSIs with DS in the range 37–56 mol % remained turbid even after cooling (Figure 1b), and the colloid dispersions remained stable for more than one week even after cooling to 0 °C. The temperature dependences of transmittance for 1 wt % aqueous solutions of IPA-PSIs with DS 76 and 37 mol % are shown in Figure 1c together with reference curves for PNPAAm for comparison. The method used to obtain the transmittance curves is given in the Supporting Information. It is apparent from this Figure that the transmittance of the aqueous solution of IPA-PSI with DS = 76 mol % changes more gradually than that of PNIPAAm, and the heating curve does not coincide with the cooling curve (as for PNIPAm). The difference between the heating and cooling curves became increasingly pronounced with decreasing DS, implying that the phase transition of

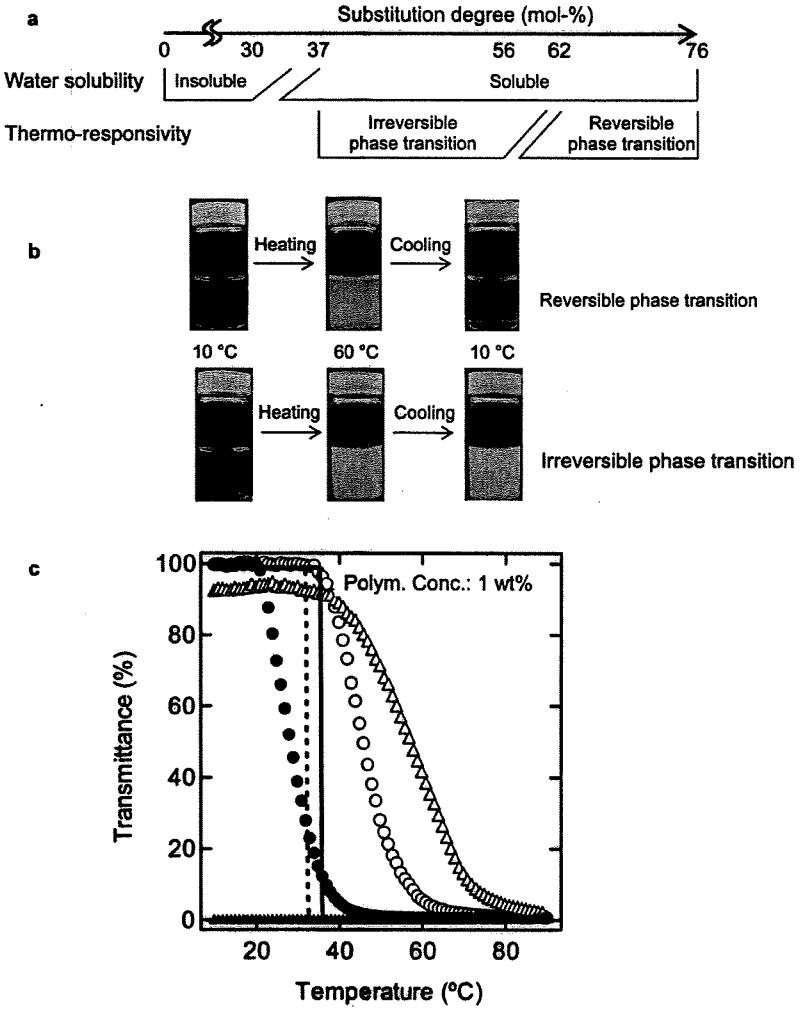

FIGURE 1. Thermoresponsiveness of aqueous solutions of IPA-PSI with various degrees of substitution (DS). (a) Effect of DS on water solubility and thermo-responsivity. (b) Change in appearance of aqueous IPA-PSI with DS = 76 (upper) and DS = 37 mol % (lower). (c) Transmittance of 1 wt % aqueous IPA-PSI solution as a function of temperature. Open triangles, heating curve for IPA-PSI with DS = 37 mol %; filled triangles, cooling curve for IPA-PSI with DS = 37 mol %; open circles, heating curve for IPA-PSI with DS = 76 mol %; filled circles, cooling curve for IPA-PSI with DS = 76 mol %; solid line, heating curve for PNIPAAm; dotted line, cooling curve for PNIPAAm.

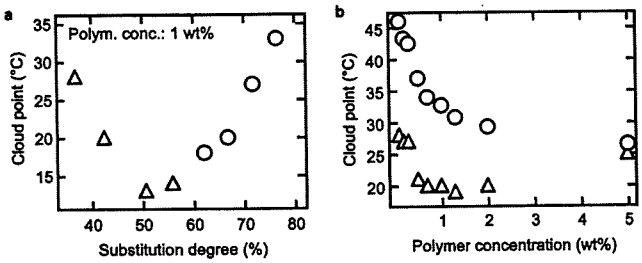

FIGURE 2. Dependence of the cloud point of aqueous IPA-PSI on DS and polymer concentration. (a) Effect of DS on cloud point of 1 wt % aqueous IPA-PSI solution. Triangles, cloud point of IPA-PSI showing irreversible phase transition; circles, cloud point of IPA-PSI showing reversible phase transition. (b) Effect of polymer concentration on cloud point of aqueous IPA-PSI solution. Triangles, DS = 43 mol %; circles, DS = 76 mol %.

IPA-PSI gradually becomes irreversible as DS decreases. The phase transition of IPA-PSI with DS < 60 mol % is irreversible, indicating that the succinimide segments in the main chain significantly affect the reversibility of the phase transition. Moreover, the sharpness of the phase transition decreased as DS decreased. This tendency is attributed to a decrease in the proportion of thermo-responsive isopropylamide units. A similar tendency has been reported for PNIPAAm copolymers with a functional group; the phase transition of PNIPAAm copolymer exhibits a more gradual transition than that of PNIPAAm homopolymer (20, 21).

The effect of DS on the cloud point of 1 wt % aqueous IPA-PSI solution is shown in Figure 2. The cloud point was strongly affected by DS and decreased as DS increased up to 50 mol %. Above that threshold, the cloud point increased as DS increased. It is reasonable to consider this peculiar tendency in two regions of DS. For IPA-PSI with DS > 50 mol %, the variation in the cloud point can be attributed to the hydrophilicity of IPA-PSI. Hydrophilic polymers form strong hydrogen bonds between the amido groups and water molecules, and require more energy to become dehydrated than do hydrophobic polymers, which implies that they have a higher cloud point. This tendency has been reported for copolymers of PNIPAAm and poly(ethylene oxide) (22–24).

For IPA-PSIs with DS < 50 mol %, the variation in the cloud point may be ascribed to increase of the number of intermolecular interaction sites. Furthermore, it seems that reducing the rigidity of the polymer backbone also accelerates intermolecular aggregation. It seems that a five-membered succinimide ring gives more rigidity compared with an aspartate unit because the glass transition temperature of the polymer is increased by decreasing DS of IPA-PSI (see Supporting Information). Consequently, for IPA-PSI with more succinimide rings to collapse, it must overcome a significant energy barrier, resulting in a higher cloud point. In addition, cloud points generally depend on the polymer concentration because aggregation is based on intermolecular interaction: it is known that PNIPAAm shows intramolecular aggregation triggered by dehydration during heating, referred to as a coil–globule transition (25). Figure 2 shows the decrease in the cloud points of IPA-PSI solutions with increasing polymer concentration.

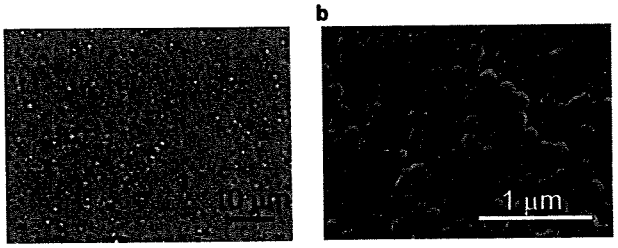

FIGURE 3. Colloid of IPA-PSI with various DS prepared by thermo-induced phase transition. (a) Optical microscopic image of 1 wt % aqueous solution of IPA-PSI with high DS, at 60 °C. (b) SEM image of IPA-PSI particulate prepared by irreversible phase transition of 1 wt % aqueous IPA-PSI solution. The particulate prepared by heating was washed by repeated centrifugation and subsequent dispersion in ultra pure water. The colloid was air-dried before observation.

The colloid induced by the phase transition of IPA-PSI was observed with an optical microscope equipped with a variable-temperature stage. Figure 3a is an image of an aqueous solution of IPA-PSI with high DS at 60 °C (above the cloud point). The figure clearly shows coacervate microdroplets, which formed thermoreversibly. By contrast, the colloid particles from IPA-PSI with low DS cannot be observed by optical microscopy, even though the solution became turbid at temperatures above the cloud point. This implies that very small colloid particles were created. The colloid particles formed by the thermoirreversible phase transition of IPA-PSI with low DS were recovered by centrifugation and resuspended in ultrapure water by agitation, confirming that the phase transition of IPA-PSI with low DS gave a solid product. Figure 3b shows a typical scanning electron microscopy image of the colloid particles prepared from IPA-PSI with low DS. The figure confirms that nanospheres several hundred nanometers in diameter were formed by the irreversible phase transition. Dynamic light scattering analysis of IPA-PSI solution after the irreversible phase transition also indicated the formation of nanospheres, in accordance with the SEM observation.

The strong dependence of cloud point on polymer concentration and the optical microscopic images provide useful information for speculation about the phase transition mechanism of IPA-PSI with high DS. Strong dependence of the cloud point on concentration has been reported for systems that show thermally induced phase separation, such as poly[(*N*,*N*-dimethylacrylamide)-*co*-(*N*-phenylacrylamide)], poly[(*N*-vinylamide)-*co*-(vinyl acetate)], and hydroxylated poly(*N*-isopropylacrylamide) (26–28). These polymers have hydrophilic segments that form hydrogen bonds with water molecules, and show no or only weak endothermic peaks at the cloud point in differential scanning calorimetry (DSC) scans. For the aqueous solution of IPA-PSI with a high DS, an endothermic peak was likewise not detected in the calorimetric study using DSC (see the Supporting Information). The origin of the endothermic peak at the cloud point is the disruption of hydrogen bonding between polymer and water molecules, and the conformational change of the polymer that results in the destruction and reconstruction of a hydrogen-bonded water network. Because of the hydrophilic polyamide backbone chain, the result obtained can be attributed to partial rather than complete dehydration.

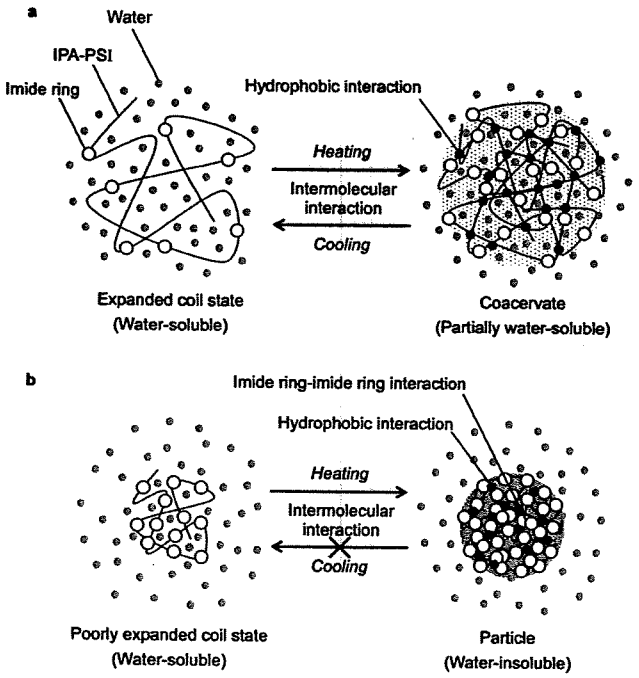

FIGURE 4. Schematic illustration of phase transition of IPA-PSI. (a) phase transition mechanism of IPA-PSI with high DS showing reversible phase transition. (b) Phase transition mechanism of IPA-PSI with low DS showing irreversible phase transition.

These considerations lead to the proposed mechanism of the reversible phase transition of IPA-PSI with high DS shown in Figure 4a. Below the cloud point, IPA-PSI with high DS is in an expanded coil state because of its high hydrophilicity. Above the cloud point, the partially dehydrated IPA-PSI molecules associate each other through hydrophobic interactions. This means that IPA-PSI with high DS involves a lot of dehydrated water molecules through the hydrophilic backbone after the phase transition, forming coacervate droplets.

By contrast, the irreversible phase transition of IPA-PSI with low DS seems to occur by a different mechanism. Because conventional thermo-responsive polymers do not show the irreversible phase transition and do not generate stable nanospheres, IPA-PSI with low DS must possess interaction forces that are sufficiently strong to stabilize particle states even below the transition temperature. The nanospheres were washed with and stored in ultrapure water. Aqueous sodium hydroxide solution was then added dropwise to the colloidal solution with gentle agitation. The turbidity of the colloidal solution gradually disappeared, resulting in a transparent solution. It is known that sodium hydroxide cleaves the succinimide unit without breaking the bond to the IPA-PSI backbone, thus producing polyaspartate. The implication is that the imide rings somehow contribute to stabilizing the particle state of IPA-PSI, and it seems that there is an interaction between the distorted pentagonal rings. This is the basis of the proposed mechanism of the irreversible phase transition, which is shown in Figure 4b. IPA-PSI can dissolve in water at low temperature, but is in a poorly expanded coil state due to its low hydrophilicity. As temperature increases, the molecule is hydrophobized by dehydration, and the hydrophobized molecules are aggregated intermolecularly by hydrophobic interaction. Above the cloud point, IPA-PSI molecules with low DS have few hydrogen-bonding interactions with water molecules and can form solid particles. The interaction between succinimide rings stabilizes the IPA-PSI conformation, resulting in stable particle even below the cloud point.

Generation of a novel biodegradable thermoresponsive polymer whose function can be altered by changing its composition, as described above, enables construction of a general purpose system. IPA-PSI can be chemically modified because the remaining succinimide units can react with nucleophiles. Therefore, IPA-PSI has the potential to replace conventional nondegradable thermo-responsive polymers in fields such as medicine, biology as well as environmental science if the phase transition temperature is tuned around 37 °C. Thus, IPA-PSI may be useful in applications such as drug delivery systems or separation technology. Furthermore IPA-PSI with low DS can be utilized in a novel process for preparing biodegradable nanospheres. This method has several advantages compared with conventional methods of preparation of biodegradable nanospheres. By contrast with most conventional methods, this simple method requires no toxic organic solvent (29, 30). The organic solvent-free process obviates the need for an organic solvent removal process, thus saving energy, reducing organic solvent waste, and eliminating hazards associated with residual organic solvent in drug, food, and environmental applications. The versatile biodegradable thermoresponsive polymer that we report here has the potential for medical, biological, and environmental applications.

Acknowledgment. This study was partly supported by a Grant-in-Aid for Scientific Research (B) (17360383) from the Ministry of Education, Culture, Sports, Science and Technology (MEXT) of Japan.

Supporting Information Available: Experimental procedure to synthesize IPA-PSI derivatives, transmittance curve, and cloud point determination, glass transition temperature, and a DSC result (PDF). This material is available free of charge via the Internet at http://pubs.acs.org.

REFERENCES AND NOTES

(1) Heskins, M.; Guillet, J. E. *J. Macromol. Sci., Chem.* **1968**, *8*, 1441.
(2) Bignotti, F.; Penco, M.; Sartore, L.; Peroni, I.; Mendichi, R.; Casolaro, M.; D' Amore, A. *Polymer* **2000**, *41*, 8247.
(3) Otero, L.; Sereno, L.; Fungo, F.; Liao, Y. L.; Lin, C. Y.; Wong, K. T. *Chem. Mater.* **2006**, *18*, 3495.
(4) Jaycox, G. D. *J. Polym. Sci., Part A: Polym. Chem.* **2004**, *42*, 566.
(5) Chung, J. E.; Yokoyama, M.; Aoyagi, T.; Sakurai, Y.; Okano, T. *J. Controlled Release* **1998**, *53*, 119.
(6) Galaev, I. Y.; Mattiasson, B. *Smart Polymers for Bioseparation and Bioprocessing*; Taylor & Francis: London, 2002.
(7) Okano, T.; Yamada, N.; Sakai, H.; Sakurai, Y. A. *J. Biomed. Mater. Res.* **1993**, *27*, 1243.
(8) Schild, H. G. *Prog. Polym. Sci.* **1992**, *17*, 163.
(9) Akashi, M.; Nakano, S.; Kishida, A. *J. Polym. Sci., Part A: Polym. Chem.* **1996**, *34*, 301.
(10) Zhang, K.; Khan, A. *Macromolecules* **1995**, *28*, 3807.
(11) Thuresson, K.; Karlstrom, G.; Lindman, B. *J. Phys. Chem.* **1995**, *99*, 3823.
(12) Yang, H.; Yan, X.; Cheng, R. *Macromol. Rapid Commun.* **2002**, *23*, 1037.

(13) Vegotsky, A , Harada, K , Fox, S W *J. Am. Chem Soc.* **1958**, *80*, 3361.
(14) Roweton, S , Huang, S J , Swift, G *J Environ Polym. Degrad* **1997**, *5*, 175.
(15) Neri, P , Antoni, G , Benvenuti, F ; Cocola, F., Gazzei, G *J Med. Chem.* **1973**, *16*, 893
(16) Nakato, T., Tomida, M , Suwa, M.; Morishima, Y , Kusuno, A , Kakuchi, T *Polym. Bull.* **2000**, *44*, 385
(17) Takeuchi, Y , Uyama, H , Tomoshige, N ; Watanabe, E , Tachibana, Y., Kobayashi, S *J Polym. Sci., Part A Polym Chem* **2006**, *44*, 671
(18) Cho, J Y , Lee, J , Gutowska, A , Tarasevich, B J ; Sohn, Y S ; Jeong, B. *J. Drug Delivery Sci. Technol.* **2006**, *15*, 71
(19) Cho, J Y., Sohn, Y S , Gutowska, A , Jeong, B *Macromol Rapid Commun.* **2004**, *25*, 964
(20) Uludag, H , Norrie, B , Kousinioris, N , Gao, T *Biotechnol. Bioeng* **2001**, *73*, 510
(21) Matsukata, M.; Aoki, T.; Sanui, K , Ogata, N ; Kikuchi, A , Sakurai, Y.; Okano, T. *Bioconjugate Chem.* **1996**, *7*, 96
(22) Priest, J H.; Murray, S L.; Nelson, R J , Hoffman, A S *ACS Symp. Ser. 350* **1987**, 255
(23) Galaev, I Y , Mattiasson, B *Enzyme Microb. Technol* **1993**, *15*, 354
(24) Ito, S *Kobunshi Ronbunshu* **1990**, *47*, 467
(25) Wang, X., Qiu, X , Wu, C *Macromolecules* **1998**, *31*, 2972
(26) Miyazaki, H ; Kataoka, K *Polymer* **1996**, *37*, 681
(27) Yamamoto, K , Serizawa, T , Akashi, M *Macromol Chem Phys.* **2003**, *204*, 1027
(28) Maeda, T.; Kanda, T.; Yonekura, Y , Yamamoto, K ; Aoyagi, T. *Biomacromolecules* **2006**, *7*, 545
(29) Cristallini, C.; Enriquez De Grassi, G , Guardines, L , Gaussmann, R *Appl. Biochem. Biotechnol.* **1984**, *10*, 267.
(30) Giunchedi, P , Conte, U *STP Pharma Sci* **1995**, *5*, 276

Materials Letters 64 (2010) 969–971

Contents lists available at ScienceDirect

Materials Letters

journal homepage: www.elsevier.com/locate/matlet

PEG–PLA nanoparticles prepared by emulsion solvent diffusion using oil-soluble and water-soluble PEG–PLA

Makoto Muranaka, Ken Hirota, Tsutomu Ono *

Department of Material and Energy Science, Graduate School of Environmental Science, Okayama University, 3-1-1 Tsushima-Naka, Okayama 700-8530, Japan

ARTICLE INFO

Article history:
Received 4 December 2009
Accepted 27 January 2010
Available online 1 February 2010

Keywords:
Nanomaterials
Polymers
Colloidal carrier
Emulsion solvent diffusion

ABSTRACT

Poly(ethylene glycol)-*block*-polylactide (PEG–PLA) nanoparticles were prepared through the oil-in-water (O/W, ethyl acetate/water) emulsion technique using oil-soluble PEG–PLA in the presence of water-soluble PEG–PLA as a surfactant. The particle diameter decreased with increasing water-soluble PEG–PLA concentration, the smallest averaged diameter was 75 nm. From these results, it was found that water-soluble PEG–PLA acted as a surfactant which prevents further coalescence of droplets. In addition, the particles diameter decreased with increasing hydrophile–lipophile balance of oil-soluble PEG–PLA in the absence of water-soluble PEG–PLA. In contrast, the particle diameter was constant in the presence of water-soluble PEG–PLA. Therefore, the capability of water-soluble PEG–PLA as a surfactant was more excellent than that of oil-soluble PEG–PLA.

1. Introduction

The colloidal carriers which are injectable drugs are classified into nanoparticles [1], micelles [2] and liposomes [3]. They are a good promising way to keep the drug activity and control its release to specific tissues. In particular, biodegradable nanoparticles, poly(ethylene glycol)-block-polylactide (PEG–PLA) nanoparticles with PEG corona has been interested as drug carriers [4–10]. A PEG layer protects the drug-loaded PLA core from their interaction with plasma proteins and phagocytic cells so that it prolongs the blood circulation times. Furthermore, the biodegradability of PLA takes an advantage in controlling drug release.

To date, PEG–PLA nanoparticles are prepared by a phase separation method [4–6], emulsion solvent evaporation [7–10]. The phase separation method has a disadvantage such as low encapsulation efficiency due to the lack of driving force for drug incorporation during the preparation of nanoparticles. On the other hand, PEG–PLA nanoparticles obtained by emulsion solvent evaporation have higher encapsulation efficiency by keeping drugs in the emulsion droplets stabilized with surfactants [11,12]. However, PEG–PLA nanoparticles with less than 180 nm in diameter have not been obtained by the technique. To accumulate drugs around cancer tumor, enhanced permeability and retention (EPR) effect is expectable if the drug carrier is less than 150 nm [13]. Therefore, it is worth developing the preparation technique of smaller PEG–PLA nanoparticles in a range of 50–100 nm for a wide range of chemotherapy.

Since surfactant is a crucial factor in the stability of emulsion and in the control of droplet diameter affecting the size of resultant nanoparticles, the selection of surfactant is most important for the emulsion solvent evaporation; besides, the available surfactant for medical use is limited in terms of toxicity and biocompatibility. Hence we considered the surfactant used in this method from the following viewpoints; (1) simply synthesized (designable), (2) no toxic, (3) biocompatible and (4) water-soluble one. Accordingly, we concluded PEG–PLA, which is the same diblock copolymer as the particle matrix except the water solubility. PEG–PLA are easily synthesized by ring-opening polymerization of lactide using poly(ethylene glycol) monomethyl ether (MeOPEG) as an initiator in the presence of stannous 2-ethylhexanoate as a catalyst [14]. In addition, the chain length of PEG and PLA is controllable by altering the molecular weight of MeOPEG used and the feed concentration of MeOPEG in the polymerization of lactide, respectively. Furthermore, organic solvent also plays a key role for this study. Although chloroform or dichloromethylene solves both PEG and PLA segments, ethyl acetate is a good solvent for only PLA segment. That is why it is possible that PEG–PLA acts as a surfactant in an ethyl acetate–water system.

In this article, we developed PEG–PLA nanoparticles less than 100 nm in diameter by emulsion solvent diffusion method using oil-soluble and water-soluble PEG–PLA. This simple process facilitates highly drug-loaded nanocarrier for cancer therapy without any residual hazardous agent.

2. Experimental

2.1. PEG–PLA synthesis

PEG–PLA was synthesized by ring-opening polymerization of D, L-lactide (Purac, Netherland) using MeOPEG (Mw=4000, NOF, Japan) as an initiator in the presence of tin(II) 2-ethylhexanoate (Wako Pure Chemical Industries, Ltd., Japan) as a catalyst. D, L-lactide, MeOPEG and a

* Corresponding author. Tel./fax: +81 86 251 8908.
E-mail address: tono@cc.okayama-u.ac.jp (T. Ono).

0167-577X/$ – see front matter © 2010 Elsevier B.V. All rights reserved.
doi:10.1016/j.matlet.2010.01.076

toluene solution of tin(II) 2-ethylhexanoate were placed into an ampoule, which was sealed under reduced pressure and immersed in an oil bath at 403 K. The polymerization was conducted for 24 h. After cooling, the reaction mixture was dissolved in chloroform and excess hexane was added. After the precipitated polymer was recovered and was washed with 2-propanol, subsequent drying under reduced pressure at 313 K was conducted.

2.2. PEG–PLA nanoparticle preparation

PEG–PLA nanoparticles were prepared by the emulsion solvent diffusion method. 2 ml of the polymer solution (60 mg of oil-soluble PEG–PLA in ethyl acetate) was emulsified by sonication (15 s; 160 W) into a 4-ml aqueous solution dissolved water-soluble PEG–PLA (0.01–5 wt.% w/v). The resultant emulsion was diluted in 100-ml aqueous solution. Finally, the nanoparticles were isolated by centrifugation at 15,000 rpm for 60 min and washed three times with water and were freeze dried.

2.3. Characterization

The weight-averaged molecular weight (*Mw*) and the polydispersity index (*Mw/Mn*) of the synthesized polymer were measured using a gel permeation chromatography (HLC 8120, Tosoh, GPC) on the basis of the polystyrene standards with tetrahydrofuran as an eluent. The morphology of PEG–PLA nanoparticles was characterized by scanning electron microscope (S-4700, Hitachi, SEM). The diameter of PEG–PLA nanoparticles in water was characterized by dynamic light scattering measurement (Zetasizer, Malvern, DLS) at 293 K.

3. Results and discussion

3.1. PEG–PLA synthesis

PEG–PLA was successfully obtained by ring-opening polymerization of D, L-lactide using MeOPEG as an initiator. The analytical results of synthesized copolymer are summarized in Table 1. To investigate the effect of the hydrophile–lipophile balance (HLB) of PEG–PLA on the diameter of PEG–PLA nanoparticles, six kinds of PEG–PLA with different HLB were synthesized.

3.2. PEG–PLA nanoparticles preparation

Fig. 1 shows the SEM image of PEG_4–PLA_{29} nanoparticles obtained by the emulsion solvent diffusion method using PEG_4–PLA_1 as a surfactant. The averaged diameter of nanoparticles was 75 nm and the diameter distribution was narrow. In addition, although the averaged-droplet diameter in the emulsion was 360 nm, the diameter became smaller when the emulsion was diluted with a great amount of aqueous solution. From these results, the nanoparticles were formed by the diffusion of ethyl acetate from the droplets to aqueous bulk solution. It was caused by high water solubility of ethyl acetate (8.7%, w/v). Furthermore, the ratio of the peak at 3.9 ppm (OCH_2CH_2 for PEG) to the one at 5.2 ppm (CH for PLA) in the ^1H NMR spectrum of PEG_4–PLA_{29} nanoparticles was almost the same as that of PEG_4–PLA_{29}.

Table 1
Molecular structures of PEG–PLA.

Code	PEG–PLA	PLA	PEG–PLA	HLB	Solubility
	Mw	*Mw*	*Mw/Mn*		
PEG_4–PLA_{36}	40,000	35,600	1.61	2.21	Oil-soluble[a]
PEG_4–PLA_{29}	33,000	28,600	1.32	2.68	Oil-soluble[a]
PEG_4–PLA_{10}	14,000	9600	1.34	6.28	Oil-soluble[a]
PEG_4–PLA_7	11,000	6600	1.14	8.23	Oil-soluble[a]
PEG_4–PLA_1	5200	800	1.07	16.6	Water-soluble[b]

[a] Highly soluble in ethyl acetate.
[b] Highly soluble in water.

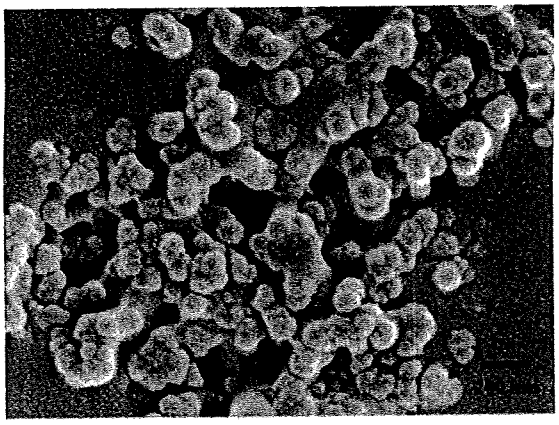

Fig. 1. SEM image of PEG_4–PLA_{29} nanoparticles prepared by the emulsion solvent diffusion method using PEG_4–PLA_1 as a surfactant; [PEG_4–PLA_{29}] = 3.3 wt.%, [PEG_4–PLA_1] = 5.0 wt.%.

It was confirmed by GPC measurement of the nanoparticles that the peak of PEG_4–PLA_1 was nothing. Therefore, this indicates that almost all PEG_4–PLA_1 are removed from the nanoparticles by the aqueous washing.

3.3. Diameter control of PEG–PLA nanoparticles

Fig. 2 shows the effect of PEG_4–PLA_1 concentration on the diameter of PEG–PLA nanoparticles. As shown this figure, the nanoparticles with a size range of 75–360 nm were obtained by altering the PEG_4–PLA_1 concentration. In addition, the particle diameter decreased with increasing the PEG_4–PLA_1 concentration. This result clarify that PEG_4–PLA_1 plays a role of surfactant which prevents further coalescence of droplets and reduces the interfacial tension between ethyl acetate and water. Moreover, the particle diameter of PEG_4–PLA_7 nanoparticles was smaller than that of PEG_4–PLA_{29} nanoparticles at low polymer concentrations. Thus, all synthesized PEG–PLA behave as a surfactant and influence the resultant particle diameter of PEG–PLA nanoparticles. Fig. 3 shows the effect of HLB of oil-soluble PEG–PLA on the diameter of PEG–PLA nanoparticles. The particle diameter decreased with increasing HLB of oil-soluble PEG–PLA in the absence of PEG_4–PLA_1. As considered above, this result proved that all PEG–PLA acted as a surfactant for the preparation of PEG–PLA nanoparticles. When using PEG_4–PLA_{36}, which has a longest PLA chain in this study, it formed stable micelles (core: PEG, shell: PLA) in ethyl acetate. Therefore, the number of PEG_4–PLA_{36} adsorbed on the interface decreased, and then the diameter of nanoparticles increased. In contrast, the particle diameter was constant in the presence of PEG_4–PLA_1. The oil-

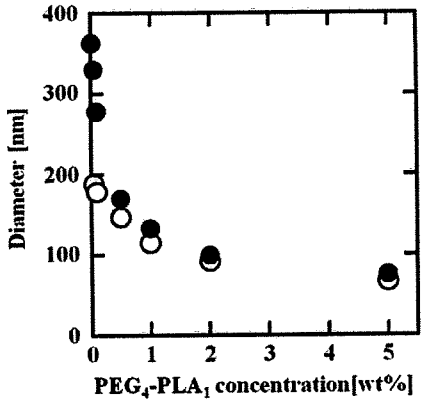

Fig. 2. The effect of PEG_4–PLA_1 concentration on the diameter of PEG–PLA nanoparticles; open key: PEG_4–PLA_7 (3.3 wt.%), closed key: PEG_4–PLA_{29} (3.3 wt.%).